

PROCESS MODELING AND FLEXIBLE MANUFACTURING OF MULTI-PHASE RESIN BASED THERMOSET AND THERMOPLASTIC PREPREG

A. Reichanadter^{1,3}, J.S. Dustin³, B. Balijepalli⁴, J.A. Mansson^{1,2,3}

¹Davidson School of Chemical Engineering, Purdue University

²School of Materials Engineering, Purdue University

³Composites Manufacturing and Simulation Center (CMSC)

⁴DOW Chemical Company

Abstract

Long cycle times, short shelf life, and processing characteristics incompatible with automation reduce the application space of traditional epoxy resin systems from consideration in high-volume automotive composite applications. A novel epoxy-based resins (VORAFUSE™) developed by DOW Chemical Company, addresses these issues with innovative chemistry and a multi-phase formulation. A common challenge in manufacturing multi-phase resin based prepreg is inconsistent material quality caused by particle filtration during the impregnation and consolidation steps. Additionally, the fiber selection can influence the quality of infiltration. For instance, A-42 carbon fiber (provided by DowAksa) has a “kidney bean” shape cross-section which will influence the compaction and filtration behavior of the fiber bed, compared to fibers with a round or elliptical profile. During a traditional thermoset impregnation process, nip rollers apply pressure to the resin initiating impregnation. However, the applied pressure also compresses the aligned fiber bed, restricting the flow channels and inducing a physical screening of the particles. This work has developed process models that identify key process parameters linked to particle filtration. Line speed, process design, and material properties play significant roles in the filtration of particles, as these parameters will influence the impregnation window. Manipulating line parameters will allow manufacturers to achieve automotive-scale production volume and economic viability for this novel resin system.

Introduction

Composite materials are attractive to industries where strength-to-weight ratio is important. The aerospace industry has long been the most notable for incorporating composite materials in their products and the composite material supply chain has largely conformed to this industry [1]. In the aerospace industry, high costs were accepted because cost savings from weight reduction and long part design lifecycle outpaced the expenses generated from low production volume. Furthermore, an aerospace part design typically remains the same for decades because of the lengthy FAA certification process [2], so the pace of new material development can be slow due to requirements of significant commitment from both the OEM and material supplier. However, new industries are embracing lightweight composite material which do not conform to previous norms, most prominently, the automotive industry. Now, the automotive industry is increasingly seeking to utilize composite components in their designs, imposing new demands on the composite materials supply chain such as significantly increased production volume, improved cycle times, material flexibility, cost, and low tack at room temperature [3].

Prepreg is an intermediate material used to construct complex composite parts. Since the 1960's, the aerospace industry has replaced metal parts with an equivalent composite analog in an effort to increase performance and decrease weight [1]. Currently, the automotive industry is

adopting composite materials in order to meet new fuel economy ratings and emissions targets imposed by the US and other governments [4]. Composites produced from prepreg are appealing to the automotive industry to meet desired strength/stiffness to weight ratios that lead to acceptable improvements in fuel efficiency. Additionally, platelet prepreg compression molding can produce Class A finishes. Platelet prepreg compression molding often achieves fiber volume fractions higher than with sheet molding compounds (SMCs), resulting in attractive new opportunities for weight savings.

In order to meet these new demands, resin manufacturers are revising resin chemistries to develop rapid cure and low tack at room temperature, such as DOW Chemical's VORAFUSE™ resins. These new formulations address many challenges that have limited composite material application in the automotive industry, however new issues in producing prepreg material have arose for these novel systems. For instance, the presence of solids can cause filtration issues during the impregnation step leading to inconsistent prepreg and ultimately poor quality parts. By modeling a two phase polymer through a prepregging process, the design and operation can be optimized for production speed and prepreg quality.

Theory and Background

The purpose of the prepregging process is to saturate the fiber bed with a polymer matrix, either thermoset or thermoplastic. This can be broken down into four key steps: 1) polymer prep, 2) heating, 3) impregnation, and 4) cooling. First the polymer must be mixed, filmed, co-mingled, or otherwise prepared so that it is compatible with the prepreg line. Then the polymer, and typically also the fiber bed, are preheated before the impregnation step. The method for polymer infusion into the fiber bed differs based on the nature of the polymer, with some common approaches including pultrusion, powder deposition, fiber co-mingling, and hot-melt. For the purposes of this study, a low tack, rapid cure thermoset saturating a bed of aligned carbon fibers will be considered undergoing a hot-melt process where the rollers are stacked on top of each other in a nip configuration and material is sent between the two rollers. Figure 1 shows a generalized hot-melt process identifying its four important manufacturing steps where the fibers enter from the left side of the figure and are pulled to the right.

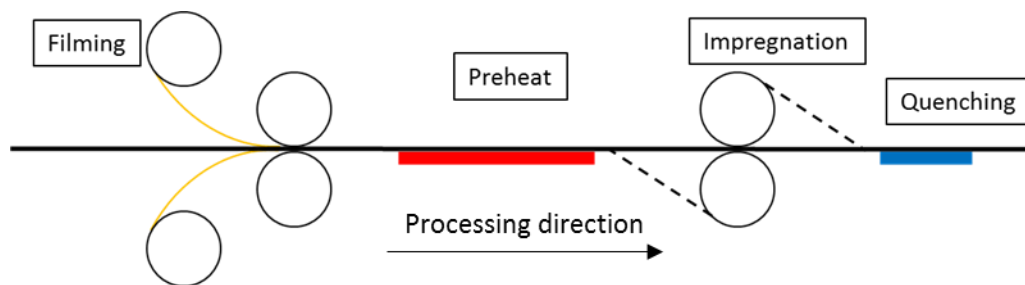


Figure 1: Generalized hot-melt prepregging process identifying the four important manufacturing steps: filming, preheating, impregnation, and quenching.

Rheo-kinetic morphology

The DOW Chemical VORAFUSE™ resins (commercially referred to as P6300 and M6400) are low tack, rapid cure epoxy based thermosetting resins. As the resin is exposed to processing temperatures during filming and impregnation, the reaction will proceed, thus it is important to track the thermal history in order to monitor the viscosity evolution and cure advancement. By studying the rheo-kinetic morphology of the resin, appropriate processing conditions can be

identified to manufacture prepreg which satisfy automotive requirements. For the purposes of this discussion, only the VORAFUSE™ M6400 will be considered.

Since the VORAFUSE™ resins were not previously studied in the literature, a complete rheo-kinetic characterization was required. This resin appeared to follow autocatalytic curing kinetics (Equation 1), and becomes diffusion limited after gelation at sufficiently cool curing conditions [5]. Where k_1 and k_2 are the observed rate constants, n and m are the partial reaction orders, and α is the degree of cure. The diffusion behavior has been observed with this resin system as shown in Figure 2, when curing conditions are below 150°C. In order to capture this behavior, a modified William-Landel-Ferry (WLF) equation (Equation 2) was used to describe the diffusion limitation by relating the cure temperature (T) to the glass transition temperature (T_g) of the curing resin. This works off the Time-Temperature-Superposition (TTS) principle, where k_{dr} , c_1 , c_2 , and T_{ref} are empirically fitted parameters. The glass transition temperature was estimated using the DiBenedetto equation (Equation 3) [6]. Where $T_{g,\infty}$ is the fully cured glass transition temperature, $T_{g,o}$ is the uncured glass transition temperature and $\lambda = \frac{T_{g,o}}{T_{g,\infty}}$. The reaction (K_i) and diffusion (K_d) rate constants were combined to define the observed rate constant k_i as described by Rabinowitch in Equation 4 [7]. Finally, the reaction rate constant is defined with the Arrhenius equation (Equation 5) where A_i is the frequency factor and E_i is the activation energy. The A_i and E_i parameters were calculated from isothermal analysis of the resin.

$$\frac{d\alpha}{dt} = (k_1 + k_2\alpha^m)(1 - \alpha)^n \quad (1)$$

$$K_d = k_{dr} e^{\frac{c_1(T-T_g(\alpha)-T_{ref})}{c_2+T-T_g(\alpha)-T_{ref}}} \quad (2)$$

$$T_g(\alpha) = \frac{T_{g,\infty} \lambda \alpha + T_{g,o}(1-\alpha)}{\lambda \alpha + 1 - \alpha} \quad (3)$$

$$\frac{1}{k_i} = \frac{1}{K_i} + \frac{1}{K_d} \quad (4)$$

$$K_i = A_i e^{-\frac{E_i}{RT}} \quad (5)$$

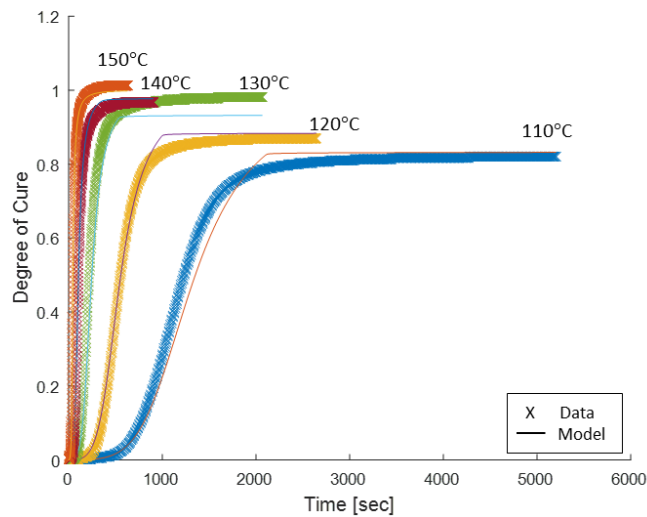


Figure 2: Various isothermal cures for VORAFUSE™ M6400 resin compared to autocatalytic with WLF diffusion model.

As with all reacting resins, the cure state will have an influence on viscosity and dictates the processing window for the material. The VORAFUSE M6400 resin's viscosity exhibited typical Arrhenius behavior until nearing gelation, where viscosity dramatically rose. The rise in viscosity associated with the cross-linking was captured through a modified WLF equation, shown in Equation 6 [8]. By pairing the Arrhenius behavior with modified WLF model (different constants from the diffusion model), the full rheological behavior could be captured, as described by Enns and Gilham [9]. A comparison between different isothermal conditions to Equation 6 are shown in Figure 3. From this comparison, it is apparent that both the first and second term in the viscosity model accurately describe the temperature dependent and cure dependent viscosity evolution.

$$\eta = \eta_{\infty} e^{\frac{E_{\eta}}{RT}} + c_3 e^{\frac{-c_1(T-T_g)}{c_2+T-T_g}} \quad (6)$$

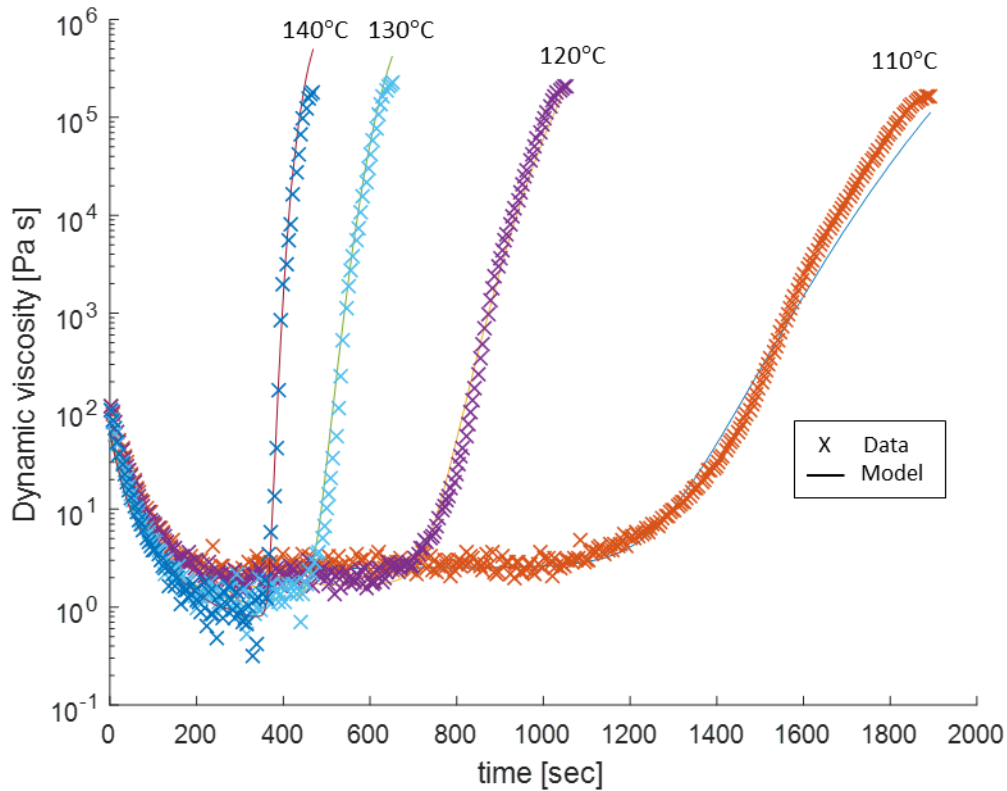


Figure 3: Various isothermal cures for VORAFUSE™ M6400 resin compared to autocatalytic model with WLF diffusion. (Samples were ramped from room temperature to the specified cure temperature).

Process modeling

Describing the movement of resin through aligned fiber beds can be approximated using Darcy's Law, shown in Equation 7 [10]. This relates the ratio of permeability (K) and pressure drop (ΔP) to the fiber bed thickness (X) and resin viscosity (η). As the driving force is increased, the fiber volume fraction (V_f) is increased. This can be approximated using the model suggested by Gutowski, shown in Equation 8 [11]. This is an empirical model which was originally developed to explain fiber bed compaction behavior in laminates. This work has been adapted to approximate the fiber bed behavior during the prepregging process. The V_a term refers to the fiber

volume fraction where the fiber bed locks and fibers are incapable of further compaction without transverse deformation. The V_o term refers to the fiber volume fraction at which a finite load can be supported. The A term is effectively the fiber bed's modulus. However, all of these terms are empirically determined and are loosely tied to the definitions provided previously. This relationship between pressure and volume fraction is important to the prepregging process. Increasing the fiber volume fraction decreases fiber spacing, which restricts the ability for material to flow through and can result in particle filtration after a critical fiber spacing has been achieved.

Since the fiber volume fraction is changing throughout the infusion step, and the permeability (K) has been known to vary with fiber volume fraction, the Carmen-Kozeny equation is used to estimate the permeability, shown in Equation 9 [10]. This permeability relationship was first derived for porous beds of aligned cylinders with a uniform radius (r_f). However, the fibers of interest (DowAksa A-42 carbon fiber) appear as “kidney bean” shapes rather than regular circles, as seen in Figure 4. Thus, an effective radius will be used for these fibers to fit pre-existing models. The ellipsoid quadratic mean radius method (Equation 10) was used to determine an equivalent fiber radius (r_f). This method approximates the fibers as ellipses and relates the long (D_l) and short (D_s) axes seen in the Figure 4 to an effective fiber radius. Moving forward, this approximation of circular cross-section for permeability and compaction may be insufficient to capture the behavior of these uniquely shaped and rotated fibers.

$$\frac{dX}{dt} = \frac{K\Delta P}{X\eta} \quad (7)$$

$$\Delta P = A \frac{\sqrt{\frac{V_f}{V_o}} - 1}{\left(\sqrt{\frac{V_a}{V_f}} - 1\right)^4} \quad (8)$$

$$K = \frac{r_f^2(1-V_f)^3}{4k_{ii}V_f^2} \quad (9)$$

$$r_f = \sqrt{\frac{D_s^2 + D_l^2}{2}} \quad (10)$$

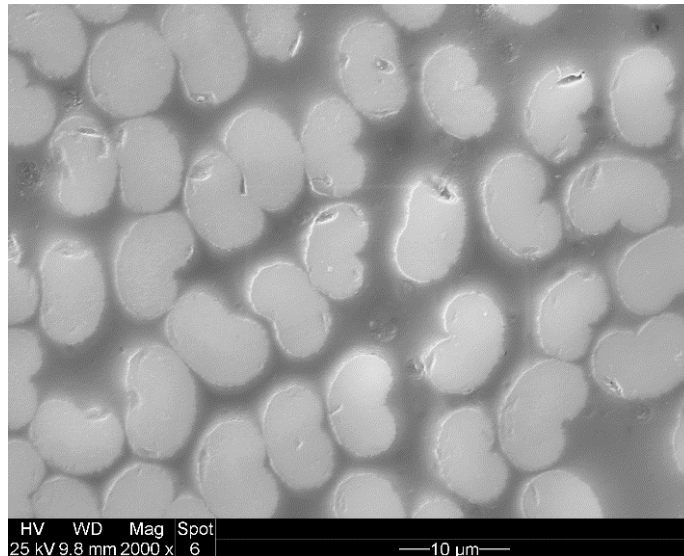


Figure 4: Micrograph of DowAksa A-42 carbon fibers showing “kidney bean” shaped cross-section.

As mentioned previously, the thermal history for thermosets must be tracked and accounted for to assess viscosity and cure state of the resin during and after the process. The heat transfer equation used can be derived from convective and conductive heat transfer equations with the integrated resultant shown in Equation 11, to approximate the temperature of the resin at any position in the process. Where T_f and T_o denote the heater and initial temperatures, respectively, x is the position in the process, and $\frac{h}{k}$ are an empirically fitted value which is functionally dependent on line speed.

$$T = T_f + (T_o - T_f)e^{-\frac{h}{k}x} \quad (11)$$

Filtration

Deep filtration has been extensively studied in isotropic, porous media. Herzig et al summarized the following particle retention sites in such media. These include surface, cavern, crevice, and constriction sites, examples of these sites are shown in Figure 5. These retentions can occur through the following mechanisms: 1) interception, 2) inertial impaction, 3) sedimentation, 4) diffusion, 5) hydrodynamic action, and 6) straining (sieving). For an in-depth discussion on these various mechanisms see References [12, 13]. From these different mechanisms, the most relevant filtration mechanism for composite manufacturing is likely straining, which will occur when the inter-fiber spacing is smaller than the particles attempting to flow through the fiber bed.

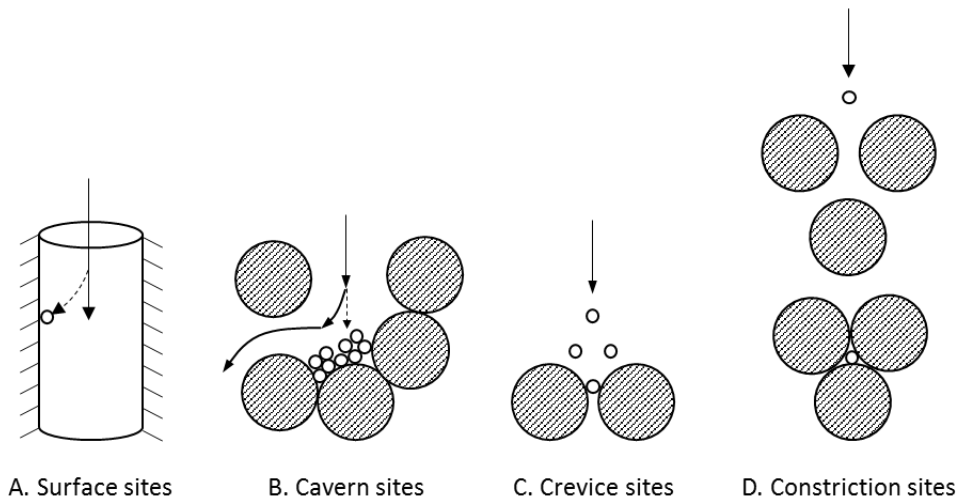


Figure 5: Types of particle retention sites in porous, isotropic media. Modified from Herzig et al [12].

Since the inter-fiber spacing will be an important factor in the particle filtration, a convenient way to describe these flow channels is needed. By assuming a hexagonally packed unit cell of either circles or ellipses (shown in Figure 6), the inter-fiber spacing (flow channel size) can be described at varying fiber volume fractions for each configuration. When approximating the fibers as circles, the minimum spacing is constant at the crevice sites, however, in the elliptic case, the crevice sites' minimum fiber spacing will vary depending on what crevice site is encountered by the particle. These crevice sites are marked in Figure 6 as A, B, C, and D, where $A=B$ and $C \geq D$. The effect of the fiber cross-section and fiber volume fraction on fiber spacing can be seen in Figure 7.

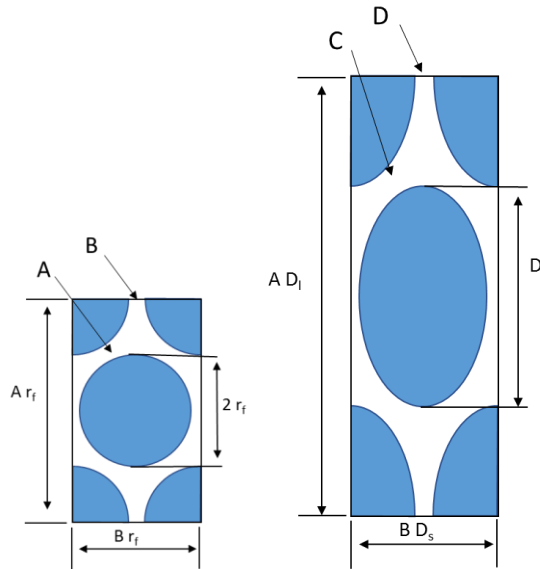


Figure 6: Hex pack unit cell for a circular cylinder (left) and elliptic cylinder (right). Where the distance between neighboring fibers is represented by A, B, C, and D. $C \geq D \geq A=B$.

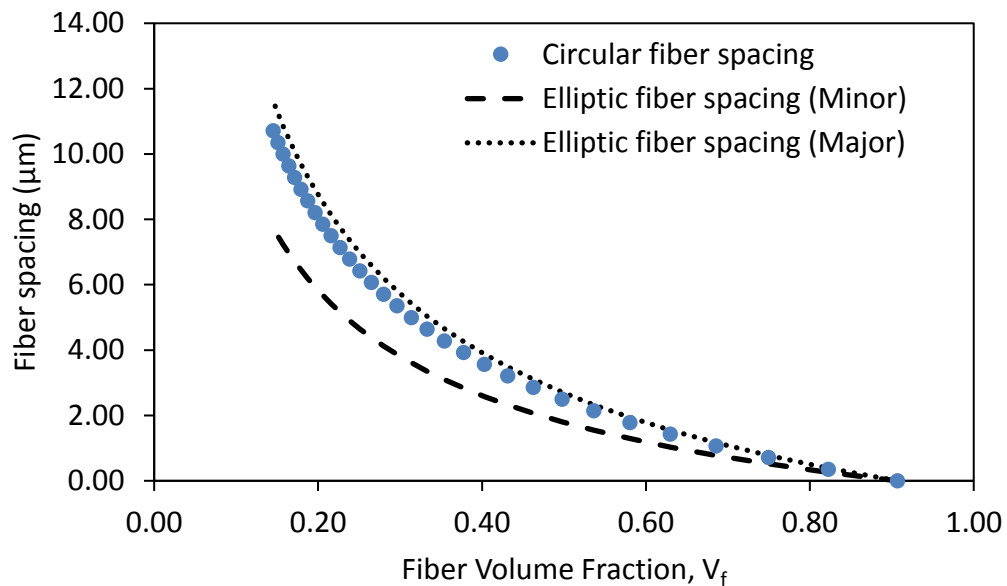


Figure 7: Fiber spacing for hexagonally packed circles and ellipses for varying fiber volume fractions.

Impregnation Modeling

The VORAFUSE™ M6400 is a multi-phased resin where the catalyst is a separate phase. These particles are approximately spherical and range from 1 - 25 μm [14]. The complete particle size distribution is shown in Figure 8. During impregnation, the inter-fiber spacing is decreased as pressure is increased which can lead to particle filtration. As particle filtration becomes more severe, the prepreg quality becomes less consistent. The degree of filtration is dependent on the fiber diameter, fiber volume fraction, and particle size. Where increasing fiber size and decreasing fiber volume fraction/particle size will reduce the degree of filtration. Additionally, the fiber shape

will impact the degree of filtration because the inter-fiber spacing will become irregular as can be seen in Figures 6 and 7. Thus the smallest flow channel, site D in Figure 6, can be considered the onset point for particles of equal or greater size to become filtered by the fiber bed. While site C in Figure 6 denotes the largest flow channel which marks the point where complete filtration will occur when particle sizes exceed the inter-fiber spacing.

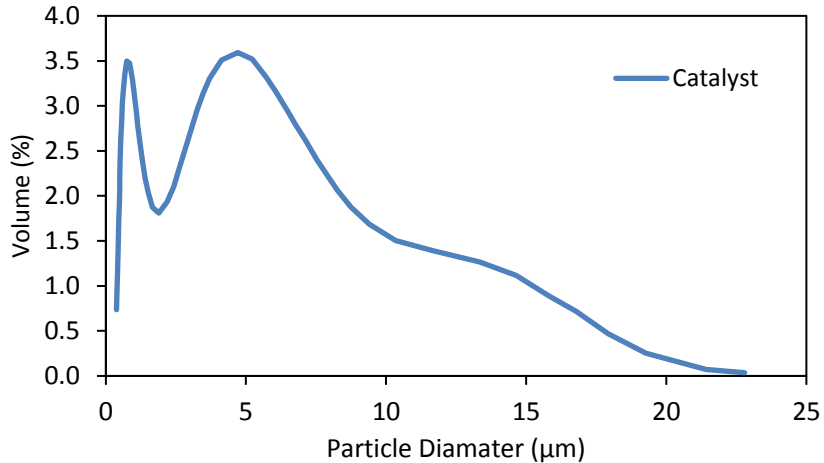


Figure 8: Catalyst particle size distribution found in VORAFUSE™ M6400 resin [14].

By capturing the heat transfer during the process, time-temperature response of the resin, fiber compaction and permeability, the prepregging process operation can be optimized for complete impregnation, cure state, and prepreg quality. For example, consider the hot-melt process indicated in Figure 1. Where the heated table and rollers are both heated to 130°C and the line is moving at 2 cm/sec then expected flow channel responses throughout the impregnation process can be monitored. This is shown in Figure 9 where the flow channels are normalized to a particle 2 μm in diameter. Thus a value ≤ 1 would indicate that particle retention will begin to occur due to the size restriction of that flow channel. In terms of prepreg quality, once the first flow channel becomes ≤ 1 , the prepreg quality will become negatively impacted. However, only once the largest flow channel is ≤ 1 , will complete filtration occur. Additionally from Figures 7 and 9, it is important to not approximate these kidney bean fibers as circles because the actual flow channels will respond quite differently. By tracking the “minor” flow channel (site C in Figure 6), the onset of filtration can be marked. This provides a quantitative metric to an otherwise qualitative outcome.

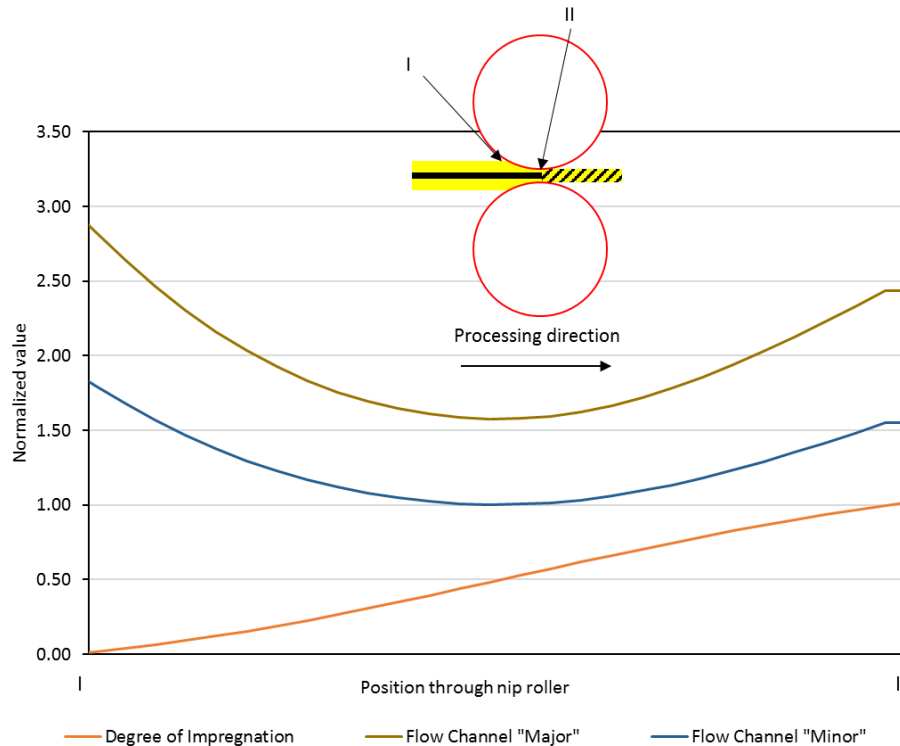


Figure 9: Predicted flow channel size for circular and elliptical fiber approximations in hexagonally packed unit cells during impregnation in a hot-melt process where point I is when the resin first makes contact with the nip roller and II is where prepreg loses contact with the nip roller. Flow channel values are normalized to a particle $2\mu\text{m}$ in diameter. Ideal flow channel refers to sites A and B in Figure 6 while minor and major flow channels refer to sites C and D, respectively.

Summary and Next Steps

After characterizing a polymer matrix and fiber bed, an impregnation process can be reasonably modeled to predict line behavior and to tune operating parameters. However, these existing models do little to provide quantitative measurements of the prepreg quality which is often measured in a quality assurance step before the line is brought up to full production. The work presented in this paper outlines a method to use relative fiber spacing as a metric to assess prepreg quality for two-phase resins. This method requires an understanding and simplification of the fiber's cross-sectional shape in order to predict prepreg quality.

At the moment, this approach to quantitatively assess prepreg quality is based off of the geometric shape and size of the fiber unit cell as the fiber bed is compacted. While this approach will capture the straining mechanism for particle retention, the method put forth does not account for the other retention mechanisms that have been observed in certain isotropic, porous beds. Thus, a validation study is needed to determine if straining is the dominant mechanism in filtration through aligned fiber beds.

Additionally, traditional impregnation processes require conveying systems to support the resin films during impregnation which leads to unnecessary waste. The thermal stability and tack free nature of this novel epoxy resin at room temperature allows for the prepreg to be manufactured through atypical (support free) routes. Filming the resin in-situ using an extrusion die with the prepreg line will eliminate the need for conveyor support during the impregnation step, which will reduce the environmental footprint of prepregging. This work is ongoing as a custom

prepreg line is being built at the Composites Manufacturing and Simulation Center (CMSC) at Purdue University to further study support free impregnation, prepreg quality, scalability, and cost effective solutions.

Acknowledgements

The authors would like to acknowledge DOW Chemical Company for providing resin, DowAksa for providing the carbon fibers. Additionally, this project was funded under the Department of Energy's Institute for Advanced Composites Manufacturing Innovation (IACMI).

Bibliography

- [1] T. Edwards. (2008) Composite Materials Revolutionise Aerospace Engineering. *Ingenia*. 24-28.
- [2] G. F. Barbosa and J. Carvalho, "Analytical model for aircraft design based on Design for Excellence (DFX) concepts and use of composite material oriented to automated processes," (in English), *International Journal of Advanced Manufacturing Technology*, Article vol. 69, no. 9-12, pp. 2333-2342, Dec 2013.
- [3] P. Martensson, D. Zenkert, and M. Akernro, "Effects of manufacturing constraints on the cost and weight efficiency of integral and differential automotive composite structures," (in English), *Composite Structures*, Article vol. 134, pp. 572-578, Dec 2015.
- [4] *Code of Federal Regulations (CFR) 2015, Title 40 - Protection of Environment, Parts 1 to 1899* (Code of Federal Regulations). Office of the Federal Register OFR, 2015.
- [5] M. R. Kamal and S. Sourour, "Kinetics And Thermal Characterization Of Thermoset Cure," (in English), *Polymer Engineering and Science*, Article vol. 13, no. 1, pp. 59-64, 1973.
- [6] A. T. Dibenedetto, "Prediction Of The Glass-Transition Temperature Of Polymers - A Model Based On The Principle Of Corresponding States," (in English), *Journal of Polymer Science Part B-Polymer Physics*, Article vol. 25, no. 9, pp. 1949-1969, Sep 1987.
- [7] E. Rabinowitch, "Collision, co-ordination, diffusion and reaction velocity in condensed systems," (in English), *Transactions of the Faraday Society*, Article vol. 33, no. 2, pp. 1225-1232, 1937.
- [8] J. B. Enns and J. K. Gillham, "Time Temperature Transformation (TTT) Cure Diagram - Modeling the Cure Behavior of Thermosets," (in English), *Journal of Applied Polymer Science*, Article vol. 28, no. 8, pp. 2567-2591, 1983.
- [9] G. Wisanrakkit and J. K. Gillham, "The Glass-Transition Temperature (T_g) As An Index Of Chemical Conversion For A High-T_g Amine Epoxy System - Chemical And Diffusion-Controlled Reaction-Kinetics," (in English), *Journal of Applied Polymer Science*, Article vol. 41, no. 11-12, pp. 2885-2929, 1990.
- [10] R. C. Lam and J. L. Kardos, "THE PERMEABILITY AND COMPRESSIBILITY OF ALIGNED AND CROSS-PLIED CARBON-FIBER BEDS DURING PROCESSING OF COMPOSITES," (in English), *Polymer Engineering and Science*, Article vol. 31, no. 14, pp. 1064-1070, Jul 1991.
- [11] T. G. Gutowski, Z. Cai, S. Bauer, D. Boucher, J. Kingery, and S. Wineman, "Consolidation

Experiments For Laminate Composites," (in English), *Journal of Composite Materials*, Article vol. 21, no. 7, pp. 650-669, Jul 1987.

- [12] J. P. Herzig, D. M. Leclerc, and P. Legoff, "FLOW OF SUSPENSIONS THROUGH POROUS MEDIA - APPLICATION TO DEEP FILTRATION," *Industrial and Engineering Chemistry*, vol. 62, no. 5, pp. 8-8, 1970.
- [13] V. Jegatheesan and S. Vigneswaran, "Deep bed filtration: Mathematical models and observations," *Critical Reviews in Environmental Science and Technology*, vol. 35, no. 6, pp. 515-569, 2005.
- [14] M. Lowe, "Information on infusion conditions," A. Reichenadter, Ed., ed, 2018.